

NACA RM L53H17a

**NACA**

# RESEARCH MEMORANDUM

PERFORMANCE CHARACTERISTICS OF A 24° STRAIGHT-OUTER-WALL  
ANNULAR-DIFFUSER—TAILPIPE COMBINATION UTILIZING  
RECTANGULAR VORTEX GENERATORS FOR FLOW CONTROL

By Charles C. Wood and James T. Higginbotham

Langley Aeronautical Laboratory  
Langley Field, Va.

**CLASSIFICATION CANCELLED**

Authority Naca Res. Mem. Date 1-10-57

By 4 RM-111  
NG 1-30-57 See

LANGLEY AERONAUTICAL LABORATORY  
RESEARCH MEMORANDUM  
LANGLEY FIELD, VIRGINIA

CLASSIFIED DOCUMENT

This material contains information affecting the National Defense of the United States within the meaning of the espionage laws, Title 18, U.S.C., Secs. 793 and 794, the transmission or revelation of which in any manner to an unauthorized person is prohibited by law.

**NATIONAL ADVISORY COMMITTEE  
FOR AERONAUTICS**

WASHINGTON  
October 6, 1953



## NATIONAL ADVISORY COMMITTEE FOR AERONAUTICS

## RESEARCH MEMORANDUM

PERFORMANCE CHARACTERISTICS OF A 24° STRAIGHT-OUTER-WALL  
ANNULAR-DIFFUSER-TAILPIPE COMBINATION UTILIZING  
RECTANGULAR VORTEX GENERATORS FOR FLOW CONTROL

By Charles C. Wood and James T. Higginbotham

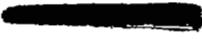
## SUMMARY

As part of an extensive subsonic diffuser research program, the performance characteristics of annular-diffuser designs applicable to turbojet afterburners are being studied. The performance of a diffuser with a 24° equivalent cone angle and having an inner body designed for uniform total-pressure loss according to Gibson has been determined with and without vortex generators for flow control. The diffuser had a constant outer-wall diameter of 21 inches and an area ratio of 1.9:1. The vortex generators used were rectangular, noncambered airfoils which were varied in span, angle setting, and location. The inlet velocity distribution corresponded to that of fully developed pipe flow. The tests were conducted with axial inlet flow and with a mean inlet whirl angle of 20.6° at a maximum inlet Mach number of 0.40 and a corresponding maximum Reynolds number of  $1.28 \times 10^6$  based on the inlet hydraulic diameter.

The best vortex-generator installations improved the diffuser static-pressure rise and downstream radial distributions without significantly altering the loss coefficients. Considering performance, geometry, and weight, the combination of the 24° diffuser and tailpipe compares very favorably, in general, with a 15° diffuser previously tested.

## INTRODUCTION

The performance characteristics of subsonic annular-diffuser designs applicable to turbojet afterburners are being studied in a research program initiated to develop short configurations which will provide stable flow, flat diffuser-exit velocity distributions, and efficient performance, all of which are important for good afterburner performance.



This is the fourth in a series of reports on this research program, which has so far depended primarily on vortex generators and on changes in the inner-wall contour for achieving the desired goals. The results of the initial investigation, in which a conical afterbody was used, are reported in reference 1. The conical afterbody was such as to produce a typical annular diffuser having an equivalent cone angle of  $15^\circ$ . This same configuration was tested in a whirling flow; results of these tests are presented in reference 2. The effect of blanking off the inner shell, and thereby creating an abrupt area expansion, is shown in reference 3 for both axial and whirling inlet flow. These investigations have served to establish reference points in the development of improved annular diffusers; the configuration with the conical inner body gave results which are considered typical, and the configuration of reference 3, while giving results which are unfavorable as was to be expected, gave important basic information necessary to proceed rationally in achieving the aforementioned goals.

The configuration reported herein was arbitrarily fixed at an equivalent conical angle of  $24^\circ$ ; the shape of the inner body was no longer conical, as was the diffuser in references 1 and 2, but was approximately parabolic, having been curved to minimize losses as recommended by Gibson in references 4 and 5. This diffuser, while being 38 percent shorter than the  $15^\circ$  diffuser, should be of sufficient length to eliminate some of the adverse effects, primarily the vena contracta formation downstream of the inner-body terminal, observed for the abrupt-expansion diffuser of reference 3.

The diffuser investigated, as well as all the other diffusers in the series, had a constant outer-wall diameter of 21 inches and an area ratio of 1.9:1. All the diffusers were tested under the same inlet conditions, a boundary layer corresponding to fully developed pipe flow, mean inlet Mach numbers up to about 0.4, and a corresponding maximum Reynolds number based on inlet hydraulic diameter of  $1.28 \times 10^6$ . The  $24^\circ$  diffuser was tested at inlet whirl angles of  $0^\circ$  and  $20.6^\circ$  with no flow control and with vortex generators consisting of NACA 0012 airfoils which were varied in span, angle setting, and location.

#### SYMBOLS

|   |  |
|---|--|
| p | static pressure  |
| H | total pressure   |
| X | whirl angle measured with respect to diffuser center line, deg |

- $\rho$  density
- $\mu$  coefficient of viscosity
- $u$  local velocity
- $U$  maximum velocity across an annular section
- $K$  constant, 0.00191
- $y$  perpendicular distance from either diffuser inner or outer wall, in.
- $X$  horizontal distance from diffuser inlet to the point determined, in.
- $r$  radius of duct, in.

$\bar{p}$  weighted static pressure,  $\frac{\int_{r_1}^{r_2} \rho u r dr}{\int_{r_1}^{r_2} \rho u r dr}$

$\bar{H}$  weighted total pressure,  $\frac{\int_{r_1}^{r_2} \rho u H r dr}{\int_{r_1}^{r_2} \rho u r dr}$

$\bar{q}_c$  impact pressure,  $\bar{H} - \bar{p}$

$\bar{\chi}$  weighted whirl angle,  $\frac{\int_{r_1}^{r_2} \rho u \chi r dr}{\int_{r_1}^{r_2} \rho u r dr}$ , deg

$\bar{u} = \frac{\int_{r_1}^{r_2} \rho u^2 dr}{\int_{r_1}^{r_2} \rho u dr}$

$D_i$  hydraulic diameter,  $\frac{4 \times \text{Cross-sectional area of duct}}{\text{Perimeter of duct}} = 0.541 \text{ ft}$

$R_i$  Reynolds number,  $\frac{\rho_i \bar{u}_i D_i}{\mu_i}$

$\frac{\overline{\Delta p}}{\bar{q}_{ci}}$  mean static-pressure coefficient,  $\frac{\bar{p} - \bar{p}_i}{\bar{q}_{ci}}$  (used for whirling inlet flow)

$\frac{\Delta p_2}{\bar{q}_{ci}}$  static-pressure coefficient,  $\frac{p_2 - \bar{p}_i}{\bar{q}_{ci}}$  (used for axial inlet flow)

$\frac{\overline{\Delta H}}{\bar{q}_{ci}}$  diffuser loss coefficient,  $\frac{\bar{H}_i - \bar{H}}{\bar{q}_{ci}}$

$\delta$  boundary-layer thickness

$\delta^*$  boundary-layer displacement thickness,  $\int_0^\delta \left(1 - \frac{u}{U}\right) dy$

$\theta$  boundary-layer momentum thickness,  $\int_0^\delta \frac{u}{U} \left(1 - \frac{u}{U}\right) dy$

$\frac{\delta^*}{\theta}$  boundary-layer shape parameter

Subscripts:

i diffuser inlet station

a axial component

1 reference to diffuser inner wall

2 reference to diffuser outer wall

## APPARATUS AND PROCEDURE

Test equipment.- A schematic drawing of the experimental setup is shown in figure 1. A more detailed drawing of the immediate area of the diffuser is shown in figure 2.

The setup consisted of an annular diffuser and tailpipe of constant outer diameter preceded by a section of annular ducting approximately 27 feet long. The diffuser had an outer diameter of 21 inches, an area ratio of 1.9:1, and an overall equivalent conical angle of expansion of  $24^\circ$ . The diffuser inner body was designed to give a uniform loss of total pressure per unit length of diffuser section, as recommended by Gibson (refs. 4 and 5), and may be represented by the equation

$$\left(\sqrt{r_{21}^2 - r_{11}^2}\right)^{-1.25} - \left(\sqrt{r_2^2 - r_1^2}\right)^{-1.25} = K(X - 4)$$

The values given by this equation agree very closely with the values obtained from direct measurements given in figure 2. The upstream annular ducting had a constant inner diameter of  $14\frac{1}{2}$  inches and an outer diameter varying between 21 and 25 inches. Air entered the test apparatus through a cylindrical screened inlet. From this chamber, air flowed through an inlet bell, through the stators, and through 27 feet of annular ducting to the diffuser inlet. The stator blades were fixed to produce an average whirl angle at the diffuser inlet of about  $21^\circ$ . The quantity of air passing through the experimental setup was controlled by a variable-speed exhauster connected far downstream of the diffuser exit.

Instrumentation.- Stream total pressures, static pressures, and whirl angles were measured by remote-control survey instruments, identical with the one shown in figure 3, at the diffuser inlet and exit stations and at the tailpipe station  $8\frac{11}{16}$  inches downstream of the diffuser exit (fig. 2). The tailpipe station corresponds to the diffuser exit for the diffuser in references 1 and 2. Flow surveys were made at only one station at a time so there were no instruments in the stream ahead of the measuring stations. These surveys were made at four equally spaced positions on the circumference of the duct at each of the survey stations. Results are based upon the average of all four circumferential positions.

Four static orifices were spaced equally around the outer wall at the diffuser inlet station, exit station, and at the tailpipe station. Static orifices extending from upstream of the diffuser inlet station

to a point approximately 30 inches downstream of the exit station were installed along a single generatrix on the outer wall. Static orifices extending from approximately the diffuser inlet station to a point approximately 5 inches upstream of the diffuser exit station were located along a single generatrix on the inner wall of the diffuser.

Small wool tufts, found to have no influencing effects on the diffuser performance, were used to observe the flow in the diffuser. These tufts were fastened along four generatrices approximately  $90^\circ$  apart on both inner and outer walls of the diffuser and were viewed through transparent windows in the outer wall of the diffuser.

Vortex generators.- Vortex-generator arrangements which had proved beneficial to the performance of a  $15^\circ$  diffuser, references 1 and 2, were used so as to permit a direct comparison between the two diffusers. Although tests were conducted in which the vortex-generator span, angle setting, and locations were varied, a systematic variation of the above variables was not made. Table I lists the vortex-generator arrangements tested. For the case of whirling inlet flow, only two arrangements were tested. One of these arrangements, arrangement 6, had large-span vortex generators on the outer wall and small-span vortex generators on the inner wall. This arrangement had been tested previously in conjunction with the  $15^\circ$  diffuser of reference 2 and was found to be equally effective at inlet whirl angles between  $0^\circ$  and  $21^\circ$ . NACA 0012 airfoil sections were used as vortex generators.

The angle setting of a vortex generator refers to the angle between the center line of the vortex generator and the diffuser center line. When whirl is present and the angle between the diffuser center line and the vortex-generator center line lies in the same quadrant as the angle between the diffuser center line and the direction of flow, the angle setting is referred to as positive; when the angle lies in different quadrants, the angle is referred to as negative. The longitudinal position of the vortex generator is referred to a plane passing through the 30-percent-chord station. The vortex generators, except when specified otherwise, were attached to the inner wall about 1 inch upstream of the cylinder-diffuser junction.

Basis of comparison of the diffuser performance.- Pressure measurements at both the diffuser exit and at the tailpipe station were made so that a comparison of the performance of this diffuser with a diffuser of equal length and with one equal in length to the  $24^\circ$  diffuser and tailpipe (for instance, the  $15^\circ$  diffuser of refs. 1 and 2) could be made.

The effectiveness of each vortex-generator arrangement on the performance of the annular diffuser has been compared on the basis of the

static-pressure coefficients  $\overline{\Delta p}/\overline{q}_{ci}$  and  $\Delta p_2/\overline{q}_{ci}$ . The mean static-pressure rise  $\overline{\Delta p}$  for the diffuser having a whirling inlet flow has been calculated as the difference between the mean static pressure at some downstream station and the mean inlet static pressure; whereas for the diffuser having an axial inlet flow, the static-pressure rise  $\Delta p_2$  has been calculated as the difference between the average readings from four static orifices equally spaced about the circumference on the outer wall at some downstream station and the mean inlet static pressure. A comparison was also made on the basis of the mean loss coefficient  $\overline{\Delta H}/\overline{q}_{ci}$  and mean whirl angle  $\overline{\chi}$ . Longitudinal distributions of static pressure  $\frac{p - \overline{p}_1}{\overline{q}_{ci}}$  and radial distributions of static pressure  $\frac{p - \overline{p}_1}{\overline{q}_{ci}}$ , total pressure  $\frac{\overline{H}_1 - H}{\overline{q}_{ci}}$ , whirl angle  $\chi$ , and velocity ratio  $u/U$  are presented for some configurations.

## RESULTS AND DISCUSSION

Before the performance of a diffuser can be evaluated, the nature of the flow entering the diffuser must be known. Data from the four survey instruments spaced about the circumference at the inlet station are presented in terms of the average total pressure, static pressure, and whirl angle in figure 4. Data are presented for an inlet pressure ratio  $\overline{p}_1/\overline{H}_{1a}$  of 0.95 for both axial flow and for a whirling inlet flow. Practically no variation in the distribution of the various parameters was observed with variation of inlet pressure ratio. The inlet velocity profiles and the associated boundary-layer properties at each of the four circumferential positions for the diffuser having axial inlet flow are presented in figure 5.

### Axial Inlet Flow

The mean diffuser loss coefficients  $\overline{\Delta H}/\overline{q}_{ci}$ , static-pressure coefficients  $\Delta p_2/\overline{q}_{ci}$ , longitudinal distributions of static pressure, and radial distributions of total pressure, static pressure, whirl angle, and velocity ratio are presented in figures 6 to 11 for axial inlet flow. Results are presented for the diffuser both with and without vortex generators. The two coefficients are presented in each case as a function of the axial inlet pressure ratio  $\overline{p}_1/\overline{H}_{1a}$ .

Flow observation.- Tufts revealed the flow along the outer wall of the diffuser to be attached and the flow along the inner wall to separate approximately 8 inches downstream of the cylinder-diffuser junction. The flow along the outer wall with control was attached and somewhat more stable than for no control, whereas the flow along the inner wall was attached several inches downstream of that observed for no control.

Diffuser performance.- A maximum static-pressure coefficient and minimum loss coefficient of 0.42 and 0.08, respectively, were observed at the diffuser exit station for the diffuser with no control (fig. 6). Corresponding coefficients at the tailpipe station were 0.51 and 0.09. The maximum static-pressure coefficient at the diffuser exit (0.42) is only 58 percent of that possible in the diffuser considering one-dimensional isentropic flow as the ideal, whereas the maximum coefficient at the tailpipe station (0.51) is 71 percent of that possible. The significant increase in static pressure in the relatively short tailpipe,  $\frac{8\frac{11}{16}}$  inches, is indicative of a rapid mixing action that is probably accelerated by the turbulence produced by the flow separation from the inner wall, which occurs approximately 5 inches upstream of the diffuser exit station. The loss of total pressure in the tailpipe, resulting from mixing action and wall friction, is approximately 12 percent of that incurred in the diffuser.

The value of loss coefficient obtained by Gibson for the diffuser shape used is approximately 0.11 when corrected for the additional friction loss of the annular diffuser. This value is greater than the measured value at the tailpipe station given in figure 6. Gibson's straight-wall-diffuser tests indicate that for a linear diameter-length variation, as obtained with a straight-wall diffuser, a loss coefficient of approximately 0.14 would result. A check of Peters' conical-diffuser tests with large inlet boundary layer (ref. 6) indicates that a  $24^\circ$  straight-wall diffuser would produce a value of  $\Delta p_2/\bar{q}_{c1}$  of about 0.33, whereas the test diffuser produced, in a comparable Mach number range, a value of  $\Delta p_2/\bar{q}_{c1}$  of about 0.39. Thus, the special shape given to the test diffuser is probably responsible for about a 27-percent decrease in loss coefficient and an 18-percent increase in pressure rise.

Figure 7, which includes results for no control as well as for all vortex-generator configurations tested for axial inlet flow, indicates vortex generators to be responsible for appreciable increases in the static-pressure coefficient, with maximum improvement realized with vortex-generator arrangement 1. This arrangement is responsible for increases of 20 and 13 percent at the diffuser exit and tailpipe stations, respectively. This increase in static-pressure coefficient, however, is

accompanied by an 18-percent increase in loss coefficient to the exit station and for no change in loss coefficient to the tailpipe station. This arrangement was also the most efficient for the diffuser of references 1 and 2. Notice that with control the performance coefficients up to the diffuser exit are approximately equal to the coefficients at the tailpipe station with no control. The same vortex-generator arrangement located 6 inches downstream (arrangement 4) has a smaller loss coefficient at the tailpipe station in the range of pressure ratio from 0.965 to 0.92 but has a somewhat larger coefficient elsewhere. Attempts to improve the performance by increasing the strength of the vortex-generator action (increased span or angle of attack) were not successful inasmuch as lower static-pressure coefficients and higher loss coefficients were obtained, as indicated in figure 7.

A comparison of the performance values for the 24° diffuser reported herein and the 15° diffuser of references 1 and 2 has been summarized in table II. The numerical values listed in the table apply for an inlet pressure ratio  $\bar{p}_i/\bar{H}_{ia}$  of 0.92; however, in most cases the variation of performance with inlet Mach number is insignificant. Values measured at the diffuser exits and at the tailpipe station are given. The 15° diffuser exit and tailpipe station are synonymous. At the diffuser exit stations the 15° diffuser shows definite superiority in static-pressure rise and velocity distribution with or without control, less total-pressure loss for the control case, and somewhat more without control. At the tailpipe station, however, there is little choice between the two diffusers with regard to static-pressure coefficients.

Radial distributions.- Figure 8 presents the radial distributions of total pressure, static pressure, whirl angle, and velocity ratio at both the diffuser exit and the tailpipe stations for the diffuser with no control and with the best control arrangement (arrangement 1). The distributions realized with the other control arrangements, available at the tailpipe station only, are very similar to those realized with arrangement 1 and have therefore not been presented. The effect of vortex generators and the tailpipe are essentially the same, both produce more uniform profiles. The velocity distribution at the diffuser exit for control is equally as favorable near the outer wall as that at the tailpipe station for no control but is by far less uniform in the region near the center of the diffuser.

The effects of diffuser length on the exit velocity distributions are shown in figure 9. The data presented are for no control and for the more efficient control arrangement. In general there are only very minor differences in the velocity profiles for the two diffusers near the outer wall; however, significant differences appear near the center portion of the diffuser. Profiles at the exit of the 15° diffuser are definitely more favorable than at the exit of the 24° diffuser. At

the tailpipe station the  $24^\circ$  diffuser has greater velocities in a region near the diffuser center line which represents approximately 15 percent of the diffuser area. This change in distribution can only be accomplished by a reduction in the maximum velocity and a shifting of the flow radially inward toward the center line. It appears, then, that for a given length for diffusion, a more favorable velocity profile can be obtained by shortening the inner body and taking advantage of the intense turbulent mixing occurring in the relatively short tailpipe. This fact becomes particularly important when it is realized that the coefficients discussed in the previous section were approximately equal for the two diffusers.

Longitudinal static-pressure distributions.- The drag loss of the vortex generators and the local acceleration due to the blocking effect of the generators produce, as shown in figure 10, lower static pressures for the first 9 inches of the outer wall and 12 inches of the inner wall. Downstream from these two points, the control case produced a definite improvement. The action of the vortex generators apparently permitted the diffuser to maintain a steep pressure gradient for about 10 inches of length as compared with about 5 inches for no control; however, for the vortex-generator case, the first inch or two was required to overcome the local pressure depression due to the vortex-generator installation.

The effect of diffuser inner-body shape on longitudinal static-pressure distributions is shown in figure 11. As the sketch in figure 11 shows, the inner body of the  $24^\circ$  diffuser, as compared with the inner body of the  $15^\circ$  diffuser which has a constant slope, has initially a more gradual rate of change of slope which becomes equal to that of the  $15^\circ$  diffuser inner body approximately 7 inches downstream; beyond this point, the rate of change is very rapid. Thus, ideally, the rate of diffusion is initially less and then much more for the  $24^\circ$  diffuser than for the  $15^\circ$  diffuser.

For no control, the favorable influence of the parabolic shape on the delay of separation from the inner wall, which was noted in tuft observations, is reflected in improved diffusion over a greater distance from the inlet station. This gain is short-lived, however, for once the flow becomes separated from the inner body, no further diffusion occurs; whereas for the  $15^\circ$  diffuser some diffusion continues and at a comparatively short distance downstream, the static-pressure coefficient equals that for the  $24^\circ$  diffuser. Thus, in the case of the  $24^\circ$  diffuser, there is little to be gained in static pressure by delaying separation.

With vortex generators, separation was prevented in the  $15^\circ$  diffuser and higher pressures were maintained along the diffuser length than for the  $24^\circ$  diffuser in which the flow separated a short distance from the downstream end of the inner body.

### Whirling Inlet Flow

In order to represent more closely the inlet condition under which this type of diffuser might be required to operate, tests were conducted with an inlet-flow whirl angle of  $20.6^\circ$ ; this value was considered as typical of a maximum value for most turbojet-afterburner installations and was believed to be adequate to obtain the effects of a whirling inlet flow on diffuser performance.

One of the conclusions of reference 2 regarding whirling flow in a diffuser was that, in order to obtain significant increases in static-pressure coefficient at this whirl angle, it was necessary to straighten the flow, thus removing the tangential kinetic energy. One vortex-generator arrangement used in conjunction with the  $15^\circ$  diffuser of reference 2 was responsible for substantial improvements in diffuser performance at inlet whirl angles up to  $20.6^\circ$ . This arrangement (arrangement 6) and one other arrangement (arrangement 5) have been used in tests of this  $24^\circ$  diffuser.

The mean loss coefficients, mean static-pressure coefficients, mean whirl angles, longitudinal distributions of static pressure, and radial distributions of total pressure, static pressure, whirl angle, and velocity ratio are presented in figures 12 to 16 for whirling inlet flow.

Flow observation.- Without vortex generators, tufts along the diffuser outer wall revealed attached flow which increased in whirl angle as the flow progressed through the diffuser, whereas tufts along the inner wall indicated attached flow over the larger portion of the inner body and indicated a very high angle of whirl, approaching  $90^\circ$ , at the diffuser exit. Vortex-generator arrangement 5 had no visible effect upon the flow on the outer wall; however, with this arrangement the flow on the inner wall remained attached over a large part of the diffuser but was observed to rotate in a direction opposite from that at the inlet and along the outer wall. Arrangement 6 created approximately axial flow along both the outer and inner walls while maintaining attached flow along the outer wall and over a large part of the inner wall.

Diffuser performance.- The mean values of static-pressure coefficient  $\overline{\Delta p}/\overline{q}_{ci}$ , loss coefficient  $\overline{\Delta H}/\overline{q}_{ci}$ , and whirl angle  $\overline{\chi}$  at both the diffuser exit and tailpipe stations for the diffuser with and without control are presented in figure 12. For no control, there are no significant changes in static-pressure coefficient or whirl angle between the two stations; however, the loss coefficient is greater at the tailpipe station over most of the speed range tested. Vortex-generator arrangement 5 results in a maximum pressure coefficient

of 0.54 and a minimum loss coefficient of 0.12 at the tailpipe station; this represents an increase in the coefficients of 9 and 53 percent, respectively, when compared with values obtained for no control. This improvement in static-pressure coefficient results from a conversion of a portion of the tangential kinetic energy to static pressure (reduction in whirl angle from  $40^\circ$  to  $20^\circ$ , see ref. 2). Arrangement 6 improved the static-pressure coefficient while increasing the loss coefficient and practically eliminating the exit whirl angle. For this arrangement, surveys were made at the diffuser exit station only; however, these surveys indicate that the static-pressure coefficient realized at this station is approximately equal to that realized at the tailpipe station when utilizing arrangement 5. For arrangement 6, substantial increases in static pressure and the establishment of a more uniform profile would probably be realized in the tailpipe because of the existence of approximately axial flows at the exit station and the expected intense turbulent mixing in the tailpipe created by flow separation from the inner body wall. The static-pressure coefficient obtained for this arrangement is approximately equal to that obtained for the diffuser having axial flow and arrangement 1; however, the loss coefficient is much greater.

A comparison of the  $15^\circ$  diffuser (ref. 2) and the  $24^\circ$  diffuser performance coefficients is given in table II. For no control the static-pressure coefficients at the exits of the  $24^\circ$  and  $15^\circ$  diffusers are equal; however, the loss coefficient of the  $24^\circ$  diffuser is approximately one-half the value for the  $15^\circ$  diffuser. With arrangement 6 the  $15^\circ$  diffuser is better in all respects. At the tailpipe stations the performance parameters for no control and for control arrangement 5 permit little choice between the two diffusers.

Radial distributions.— The distributions of total pressure and static pressure, expressed, respectively, in terms  $\frac{\bar{H}_1 - H}{\bar{q}_{ci}}$  and  $\frac{p - \bar{p}_1}{\bar{q}_{ci}}$ , whirl angle  $\chi$ , and velocity ratio  $u/U$  are presented at both the diffuser exit and tailpipe stations with control and no control in figure 13. For no control the total-pressure losses near the outer wall are smaller, the static pressures are much greater, and the whirl angles are smaller than near the inner wall. Comparison of the no-control curves at the diffuser exit station with those at the tailpipe station in a region near the outer wall indicates that the total pressures are greater, static pressures are less, and whirl angles are less than at the tailpipe station. The opposite is true near the inner wall.

The effect of vortex-generator arrangement 5 was to reduce the total- and static-pressure variation and to alter the whirl-angle distribution in a manner such that the flow near the inner wall whirled in a direction opposite to that near the outer wall. The velocity

profile for the diffuser with this arrangement is more favorable near the outer wall and less favorable near the inner wall than the profile of the diffuser with no control. Arrangement 6 had somewhat the same effect as arrangement 5 except the whirl angle was approximately constant near  $0^\circ$  across the duct. It should be noted that essentially all of the tangential kinetic energy was removed by this arrangement.

A comparison of the  $15^\circ$  and  $24^\circ$  diffuser velocity profiles at both the diffuser exit and the tailpipe stations for control and no control is given in figure 14. The velocity profiles at the exit station of the  $24^\circ$  diffuser are somewhat more irregular than at the exit of the  $15^\circ$  diffuser. The profiles of the two diffusers at the tailpipe station are almost identical. At the tailpipe station the profiles observed with no control are more uniform than those for axial flow with vortex generators; however, the radial total and static-pressure coefficients for axial flow, discussed earlier for the  $24^\circ$  diffuser and in reference 2 for the  $15^\circ$  diffuser, are more uniform than noted for whirling flows.

Longitudinal static-pressure distributions.- The distributions of static pressure, shown in figure 15, indicate a local acceleration of the flow at the cylinder-diffuser junction. With no control a maximum pressure is observed to occur on the inner wall 13 inches from the inlet station. The decrease in pressure downstream from this point results from an increase in whirl motion. The effect of vortex-generator arrangement 5 on static pressures along the outer wall is negligible, whereas the effect on the inner wall is to increase the rate of change along the wall and thus give a higher final pressure. Arrangement 6 gives slightly lower pressures along the outer wall and correspondingly higher pressures along the inner wall than did arrangement 5.

A comparison of the longitudinal static-pressure coefficients on the inner and outer walls of the  $15^\circ$  and  $24^\circ$  diffusers in a whirling flow is presented in figure 16. Without vortex generators, there is little difference between the two diffusers. Both show only a small rise in static pressure along the inner body. With vortex generators, diffusion is a little better in the  $15^\circ$  diffuser. The vortex generators have also equalized the diffusion along both surfaces for both diffusers.

## CONCLUSIONS

The following conclusions are drawn as to the performance and the influence of vortex generators on performance of an annular straight-outer-wall diffuser and tailpipe having an outer diameter of 21 inches,

an area ratio of 1.9:1, and a  $24^\circ$  overall equivalent conical expansion angle. The center body of this diffuser was designed to give a constant loss of total pressure per unit length of diffuser. The diffuser was tested with fully developed pipe flow at the inlet for two inlet angles of whirl,  $0^\circ$  and  $20.6^\circ$ .

1. With axial inlet flow and no control, the diffuser performed relatively inefficiently compared to estimates based on one-dimensional analysis.

2. For axial inlet flow and no control, the total-pressure loss and static-pressure rise of this diffuser were better than those of an equivalent-length diffuser having a conical inner body.

3. With control the performance coefficients up to the diffuser exit were approximately equal to those realized at the tailpipe station with no control.

4. The best vortex-generator installation improved the static-pressure coefficient and downstream radial distributions without significantly altering the loss coefficient.

5. For  $20.6^\circ$  whirling inlet flow and no control, there was no noticeable improvement in the static-pressure coefficient between the diffuser exit and tailpipe stations; however, the loss coefficient increased significantly and the velocity profile was greatly improved.

6. Each vortex-generator configuration increased the static pressure and loss coefficients, greatly decreased the exit whirl angle, and established less uniform velocity profiles.

7. Considering performance, geometry, and weight, the combination of the  $24^\circ$  diffuser and tailpipe compares very favorably in general to the  $15^\circ$  diffuser tested previously.

Langley Aeronautical Laboratory,  
National Advisory Committee for Aeronautics,  
Langley Field, Va., August 14, 1953.

## REFERENCES

1. Wood, Charles C.: Preliminary Investigation of the Effects of Rectangular Vortex Generators on the Performance of a Short 1.9:1 Straight-Wall Annular Diffuser. NACA RM L51G09, 1951.
2. Wood, Charles C., and Higginbotham, James T.: The Influence of Vortex Generators on the Performance of a Short 1.9:1 Straight-Wall Annular Diffuser With a Whirling Inlet Flow. NACA RM L52L01a, 1953.
3. Wood, Charles C., and Higginbotham, James T.: Flow Diffusion in a Constant-Diameter Duct Downstream of an Abruptly Terminated Center Body. NACA RM L53D23, 1953.
4. Gibson, A. H.: On the Flow of Water Through Pipes and Passages Having Converging or Diverging Boundaries. Proc. Roy. Soc. (London), ser. A, vol. 83, no. 563, Mar. 2, 1910, pp. 366-378.
5. Gibson, A. H.: On the Resistance to Flow of Water Through Pipes or Passages Having Divergent Boundaries. Trans. Roy. Soc. Edinburgh, vol. 48, part I, no. 5, 1911, pp. 97-113.
6. Peters, H.: Conversion of Energy in Cross-Sectional Divergences Under Different Conditions of Inflow. NACA TM 737, 1934.

TABLE I

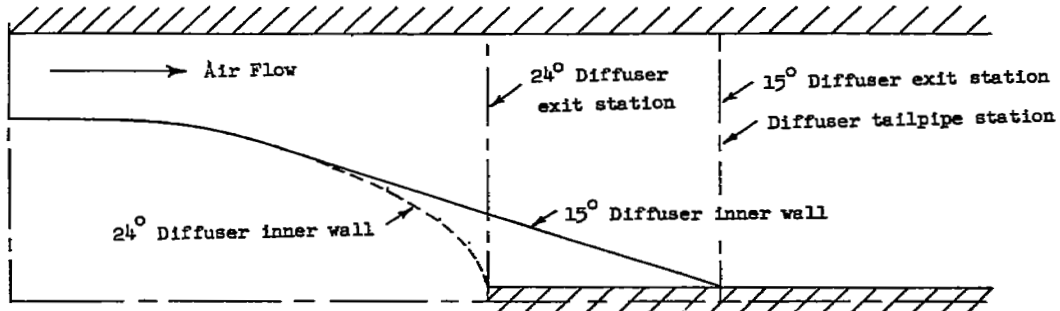
## VORTEX-GENERATOR ARRANGEMENTS TESTED

[Twenty-four 3-inch-chord generators having NACA 0012 airfoil sections]

| Arrangement | Span, in.       | Setting         | Diffuser wall | Angle setting of adjacent airfoils, deg | Inlet whirl angle, deg | Location upstream (+) or downstream (-) from cylinder-diffuser junction, in. |
|-------------|-----------------|-----------------|---------------|---|------------------------|--|
| 1           | $\frac{1}{2}$   | Counterrotating | Inner         | $\pm 15$                                | 0                      | +1   |
| 2           | $\frac{1}{2}$   | -----do-----    | --do-         | $\pm 23$                                | 0                      | +1   |
| 3           | 1               | -----do-----    | --do-         | $\pm 15$                                | 0                      | +1   |
| 4           | $\frac{1}{2}$   | -----do-----    | --do-         | $\pm 15$                                | 0                      | -5   |
| 5           | $1\frac{9}{16}$ | Corotating      | --do-         | -4                                      | 20.6                   | +1   |
| 6           | $\frac{1}{2}$   | Counterrotating | --do-         | $\pm 15$                                | 20.6                   | +1   |
|             | $\frac{3}{8}$   | Corotating      | Outer         | 0                                       | 20.6                   | +2   |


 NACA

TABLE II  
COMPARISON OF PERFORMANCE OF THE 24° DIFFUSER WITH  
THAT OF THE 15° DIFFUSER OF REFERENCE 2



| Vortex-generator arrangement | Diffuser angle, deg | Station                | $\frac{\Delta p}{\bar{u}_{c1}}$ | $\frac{\overline{\Delta H}}{\bar{u}_{c1}}$ | $\bar{x}$ , deg |
|------------------------------|---------------------|------------------------|---------------------------------|--|-----------------|
| Axial inlet flow             |                     |                        |                                 |  |                 |
| None                         | 24                  | Diffuser exit tailpipe | 0.42<br>.51                     | 0.08<br>.09                                | ---<br>---      |
|                              | 15                  | Diffuser exit tailpipe | .50<br>.50                      | .10<br>.10                                 | ---<br>---      |
| 1                            | 24                  | Diffuser exit tailpipe | .50<br>.58                      | .09<br>.09                                 | ---<br>---      |
|                              | 15                  | Diffuser exit tailpipe | .61<br>.61                      | .04<br>.04                                 | ---<br>---      |
| 20.6° whirling inlet flow    |                     |                        |                                 |  |                 |
| None                         | 24                  | Diffuser exit tailpipe | 0.48<br>.49                     | 0.03<br>.07                                | 38<br>40        |
|                              | 15                  | Diffuser exit tailpipe | .48<br>.48                      | .07<br>.07                                 | 42<br>42        |
| 5                            | 24                  | Diffuser exit tailpipe | ----<br>.54                     | ----<br>.11                                | ---<br>19       |
|                              | 15                  | Diffuser exit tailpipe | .53<br>.53                      | .12<br>.12                                 | 25<br>25        |
| 6                            | 24                  | Diffuser exit tailpipe | .52<br>----                     | .15<br>----                                | 1<br>---        |
|                              | 15                  | Diffuser exit tailpipe | .58<br>.58                      | .09<br>.09                                 | 5<br>5          |

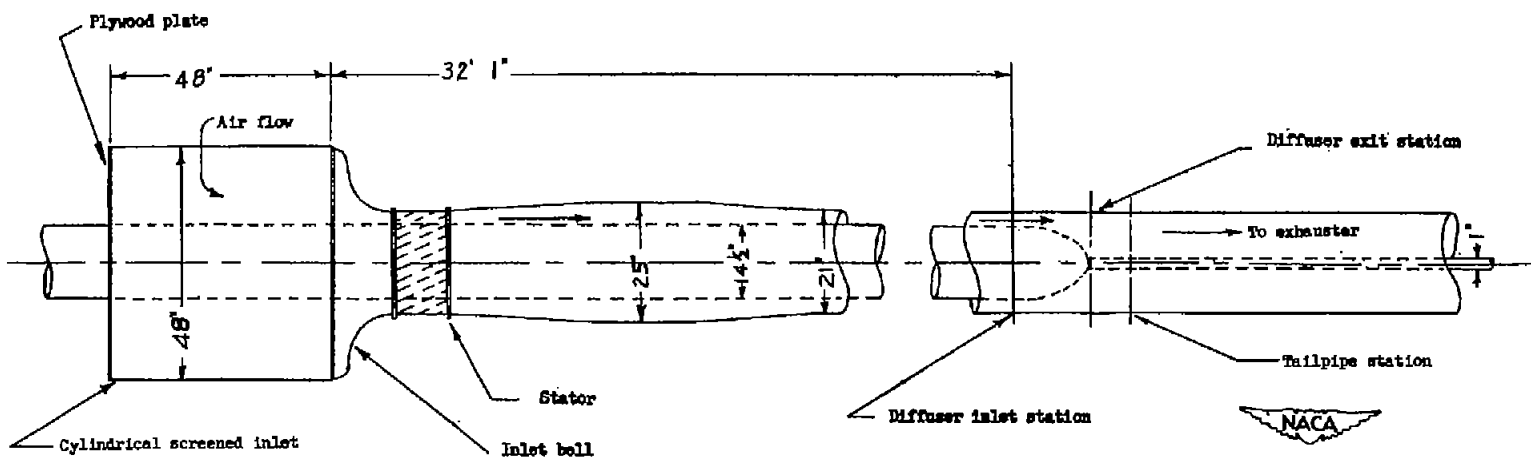


Figure 1.- Schematic diagram of experimental setup.

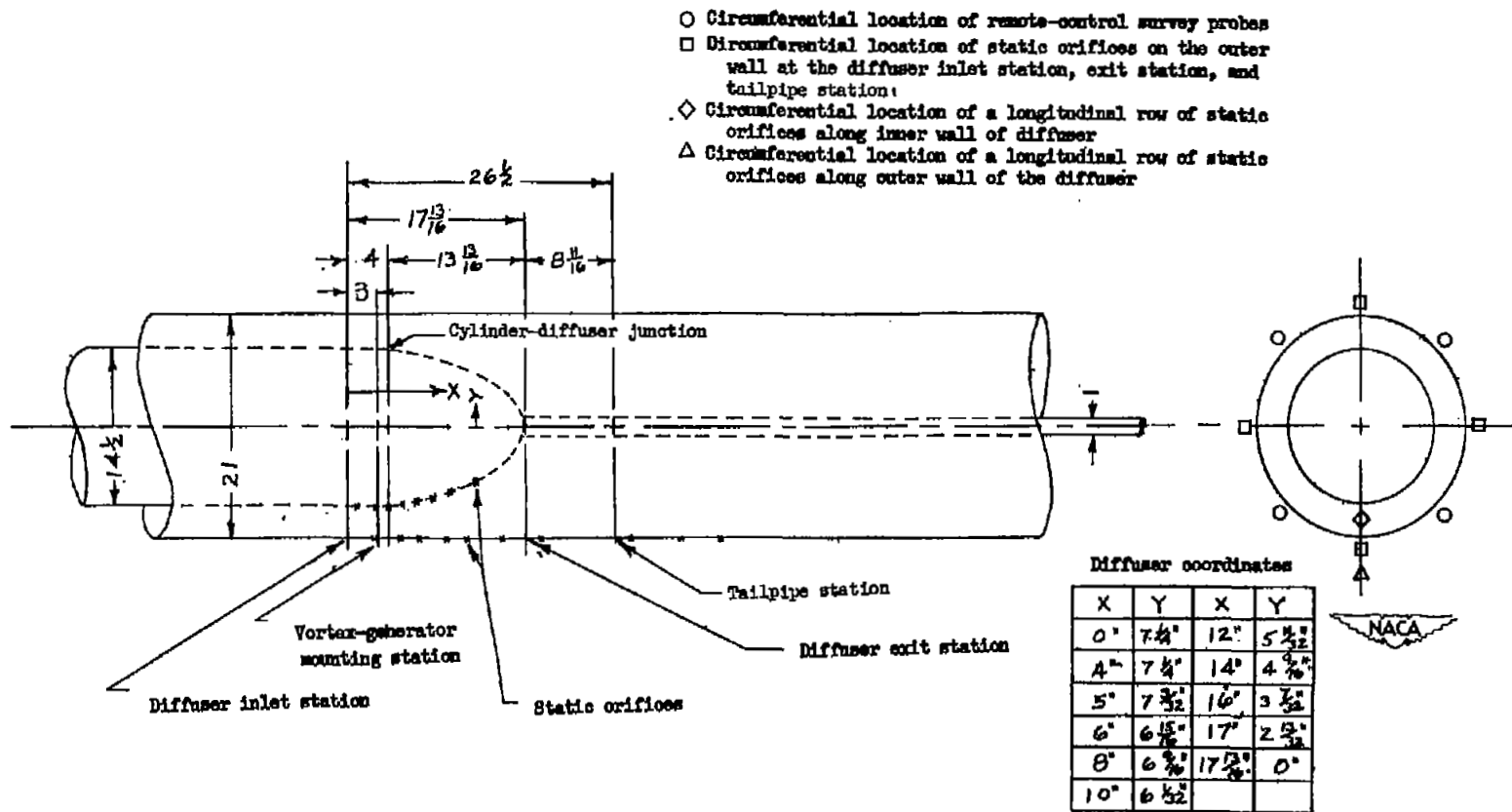


Figure 2.- Schematic diagram of the diffuser tested. All dimensions are in inches.

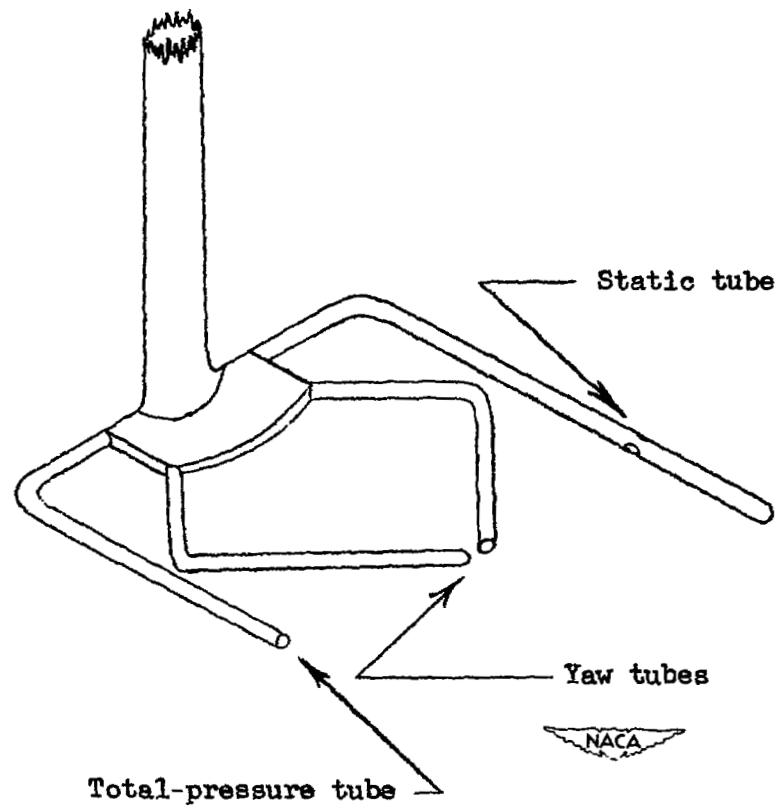


Figure 3.- Sketch of a typical survey instrument.

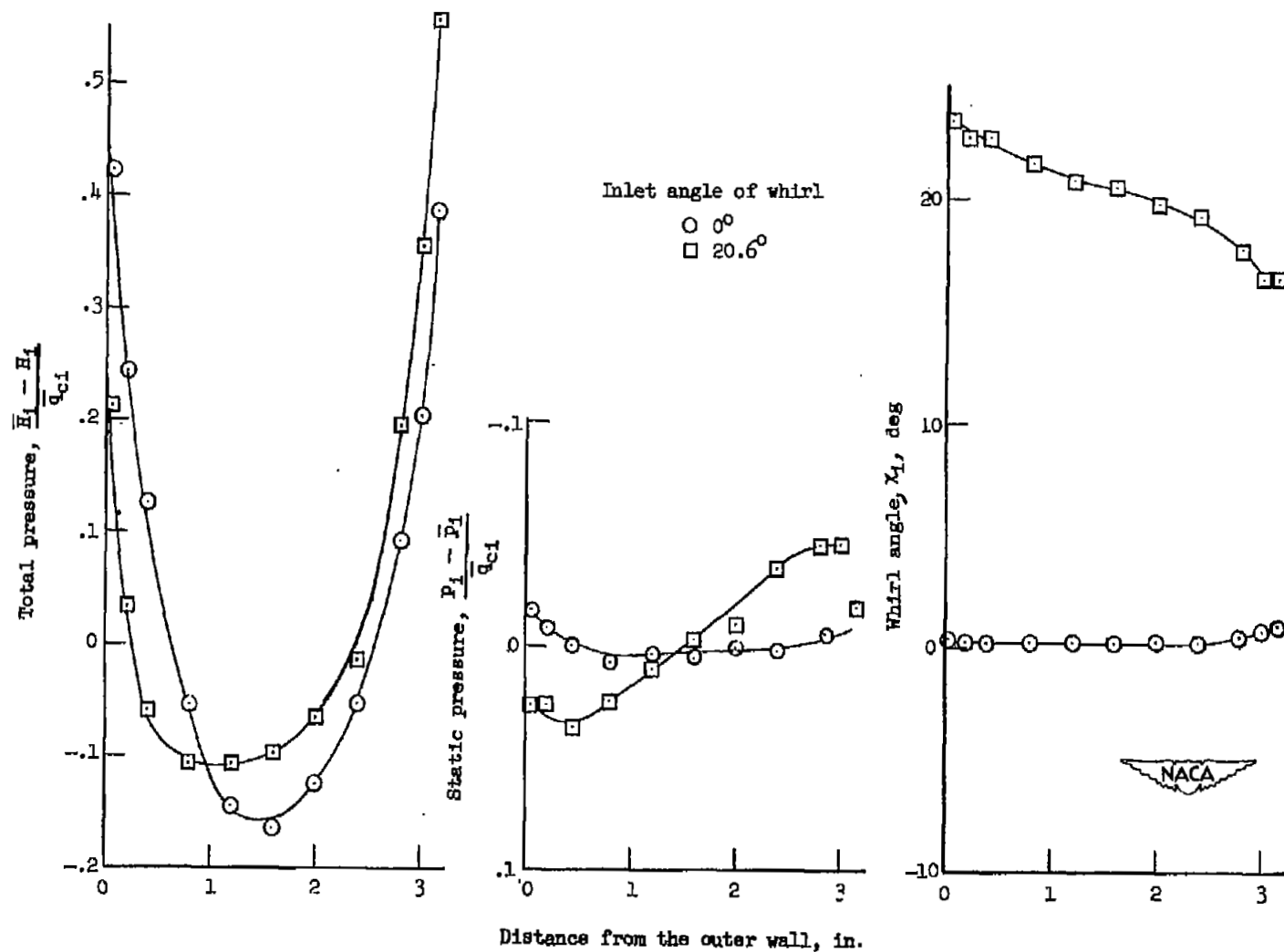


Figure 4.- Radial variations of total pressure, static pressure, and whirl angle at the diffuser inlet for two inlet-whirl angles.  
 $\frac{P_1}{\bar{H}_{1a}} \approx 0.95$ .

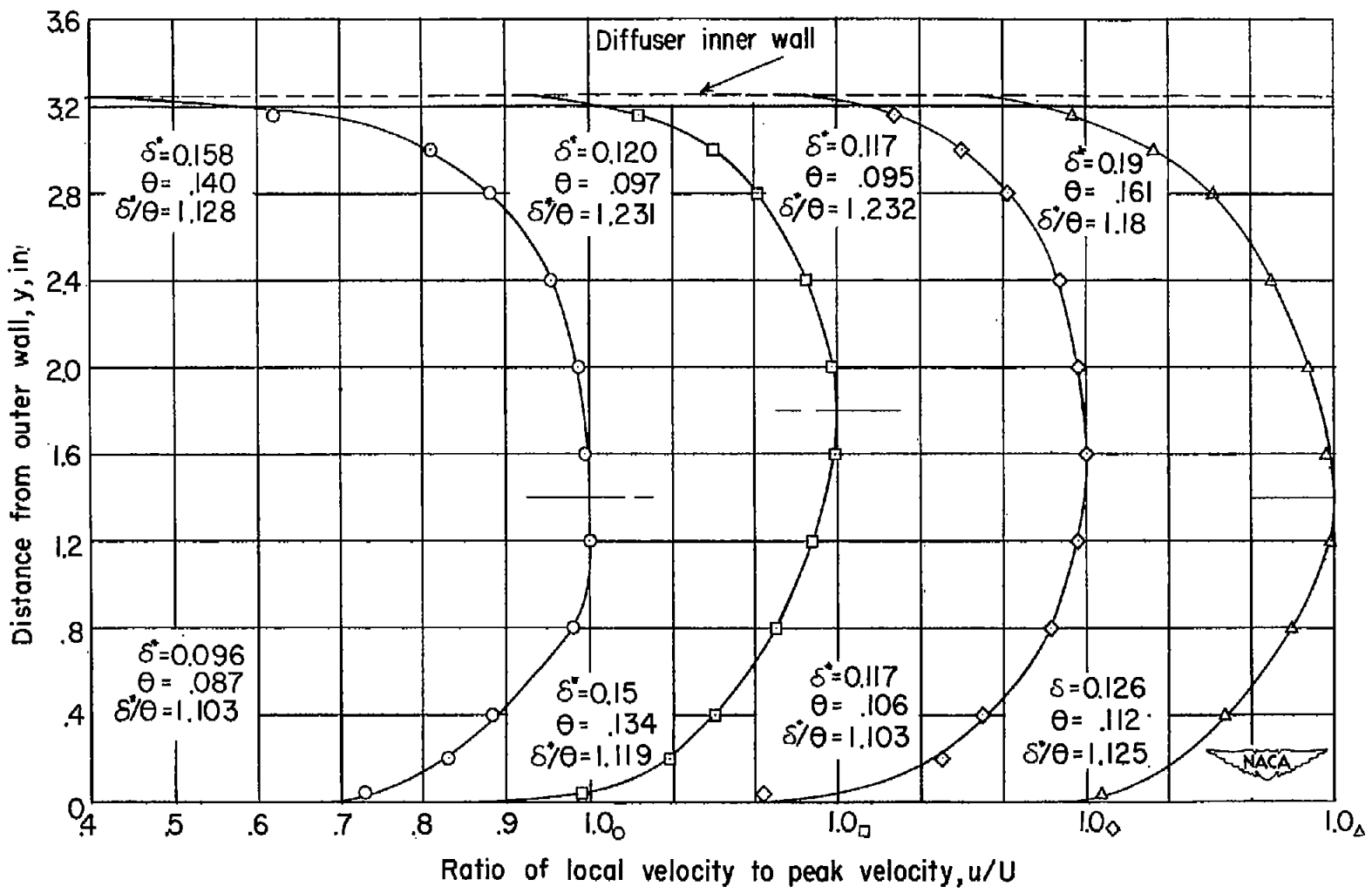


Figure 5.- Velocity profiles at four equally spaced sections around the diffuser inlet station.  $\bar{x}_1 = 0^0$ ;  $\bar{p}_1/\bar{p}_{1a} \approx 0.95$ .

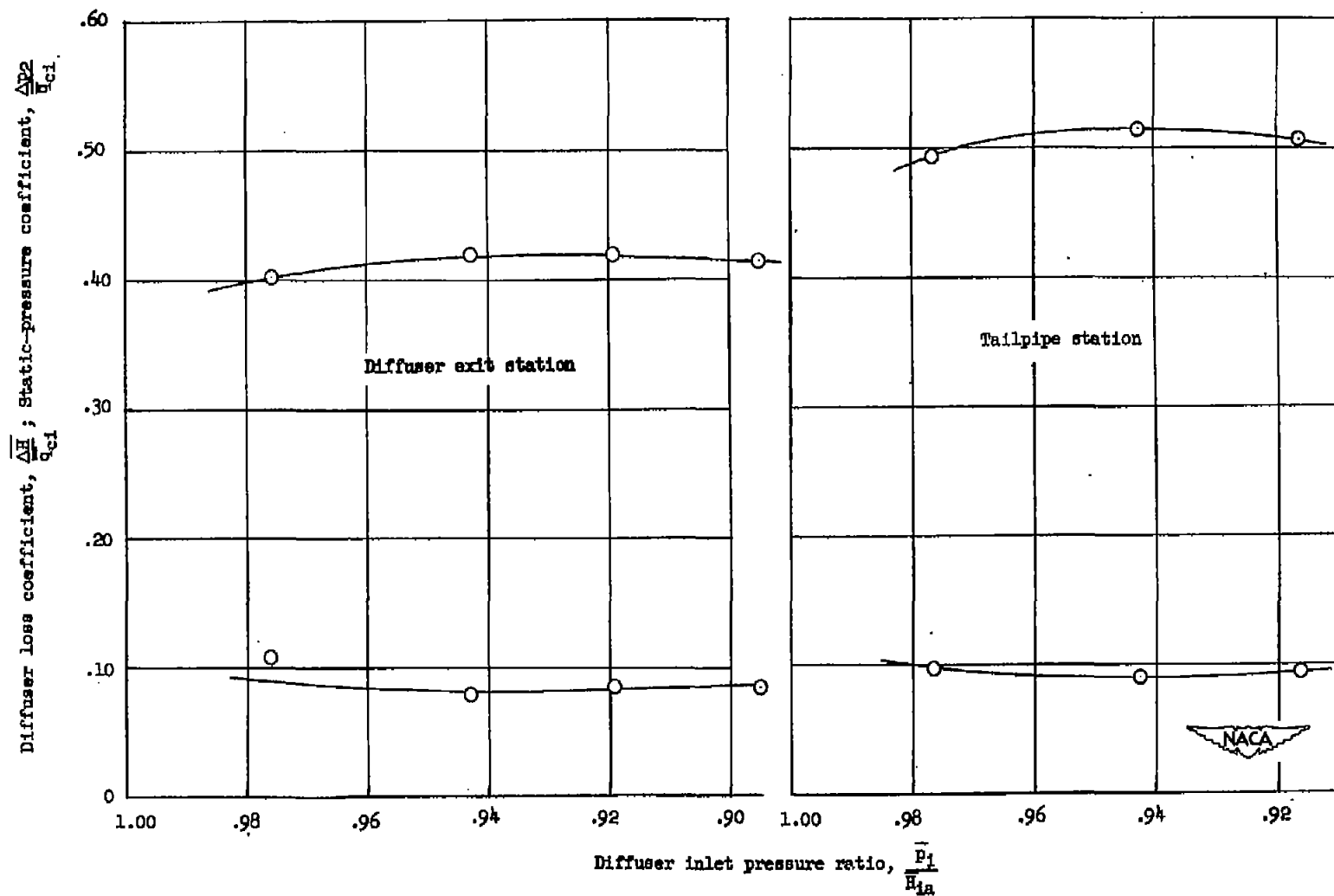


Figure 6.- Variation of static-pressure coefficient and loss coefficient with inlet pressure ratio for the diffuser with no control.  $\alpha_1 = 0^\circ$ .

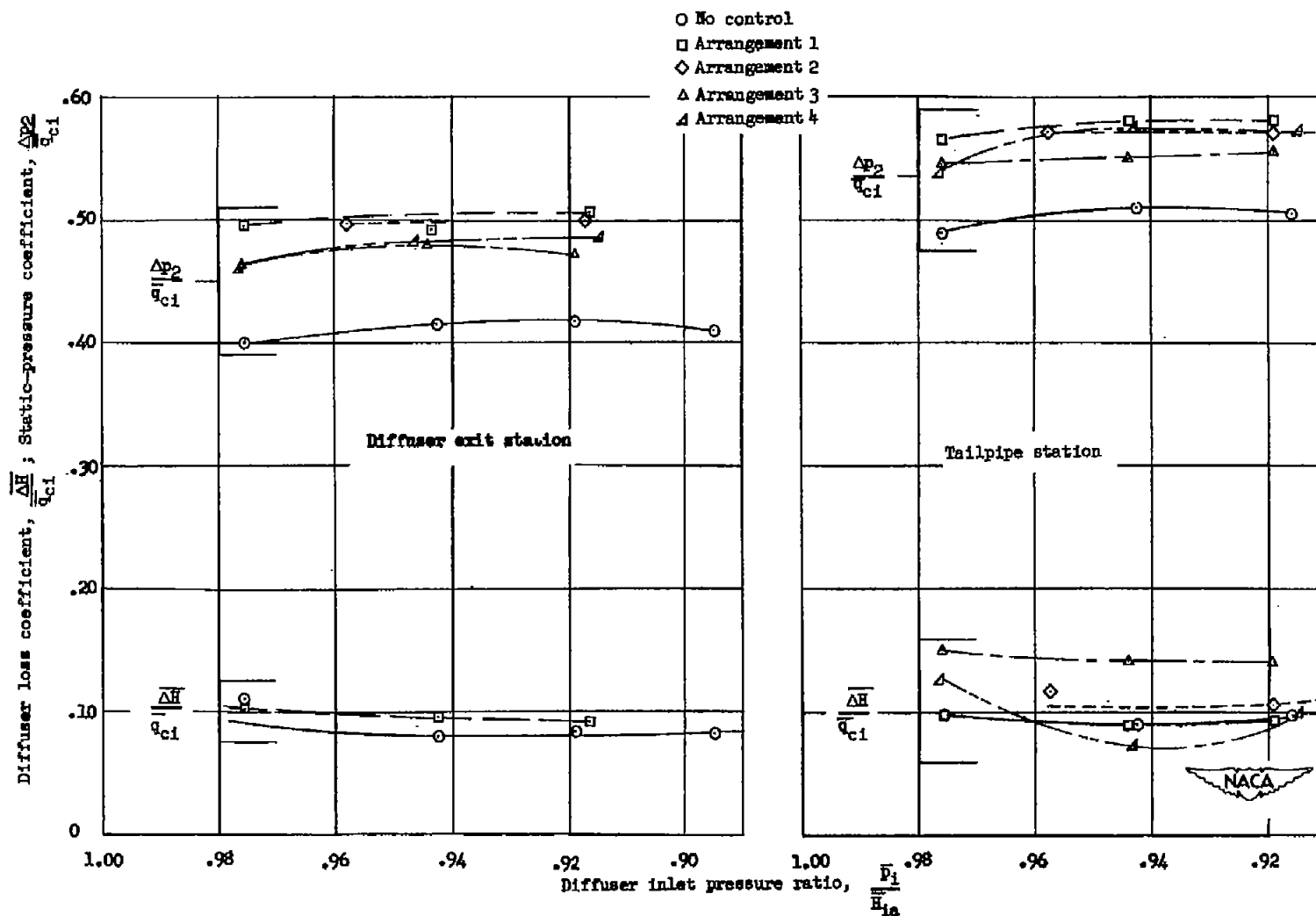


Figure 7.- Variation of static-pressure coefficient and loss coefficient with inlet pressure ratio.  $\bar{\alpha}_1 = 0^\circ$ .

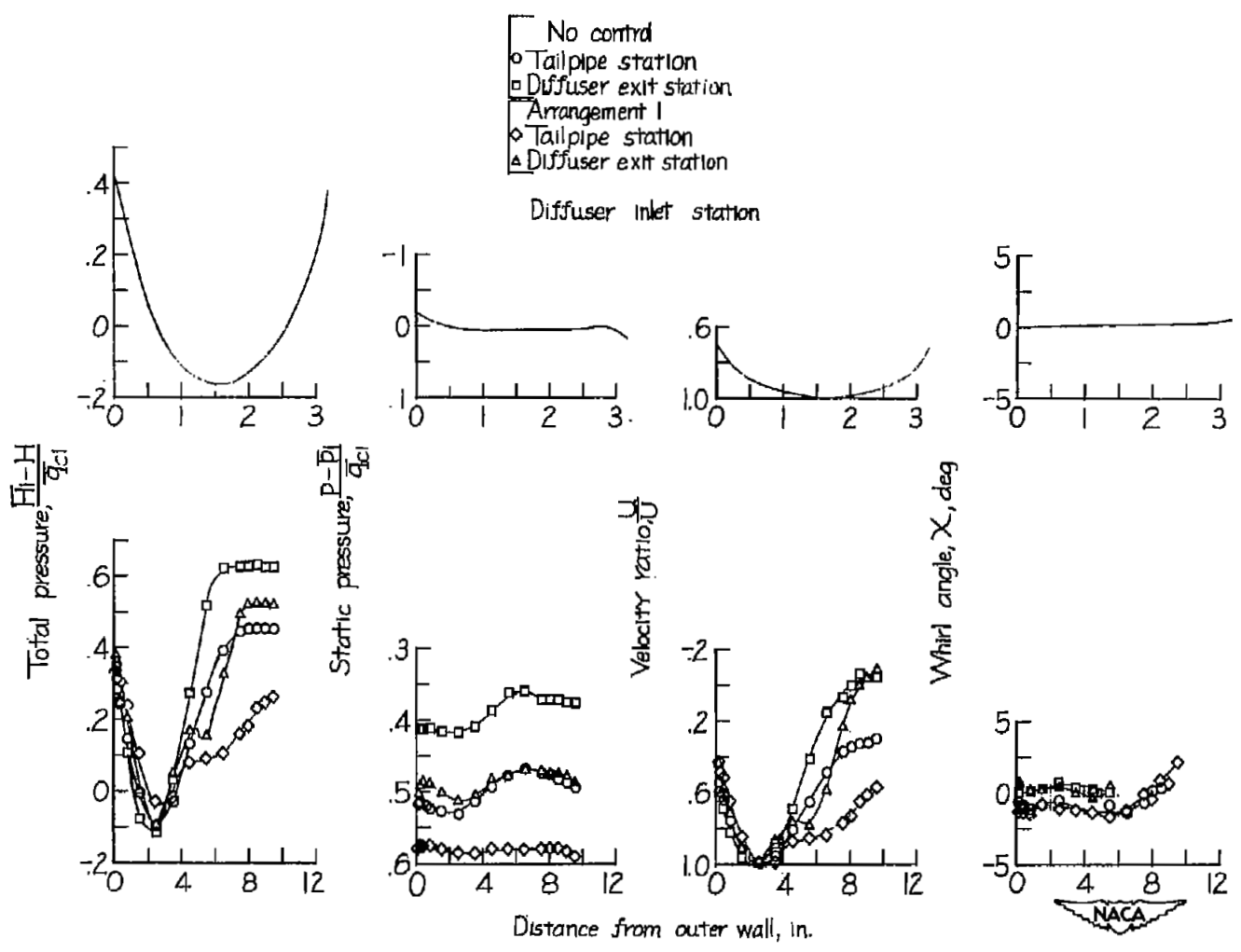


Figure 8.- Radial variation of total pressure, static pressure, velocity ratio, and whirl angle at both the tailpipe and diffuser exit stations.  $\bar{\chi}_1 = 0^\circ$ ;  $\bar{p}_1/\bar{H}_{1a} \approx 0.95$ .

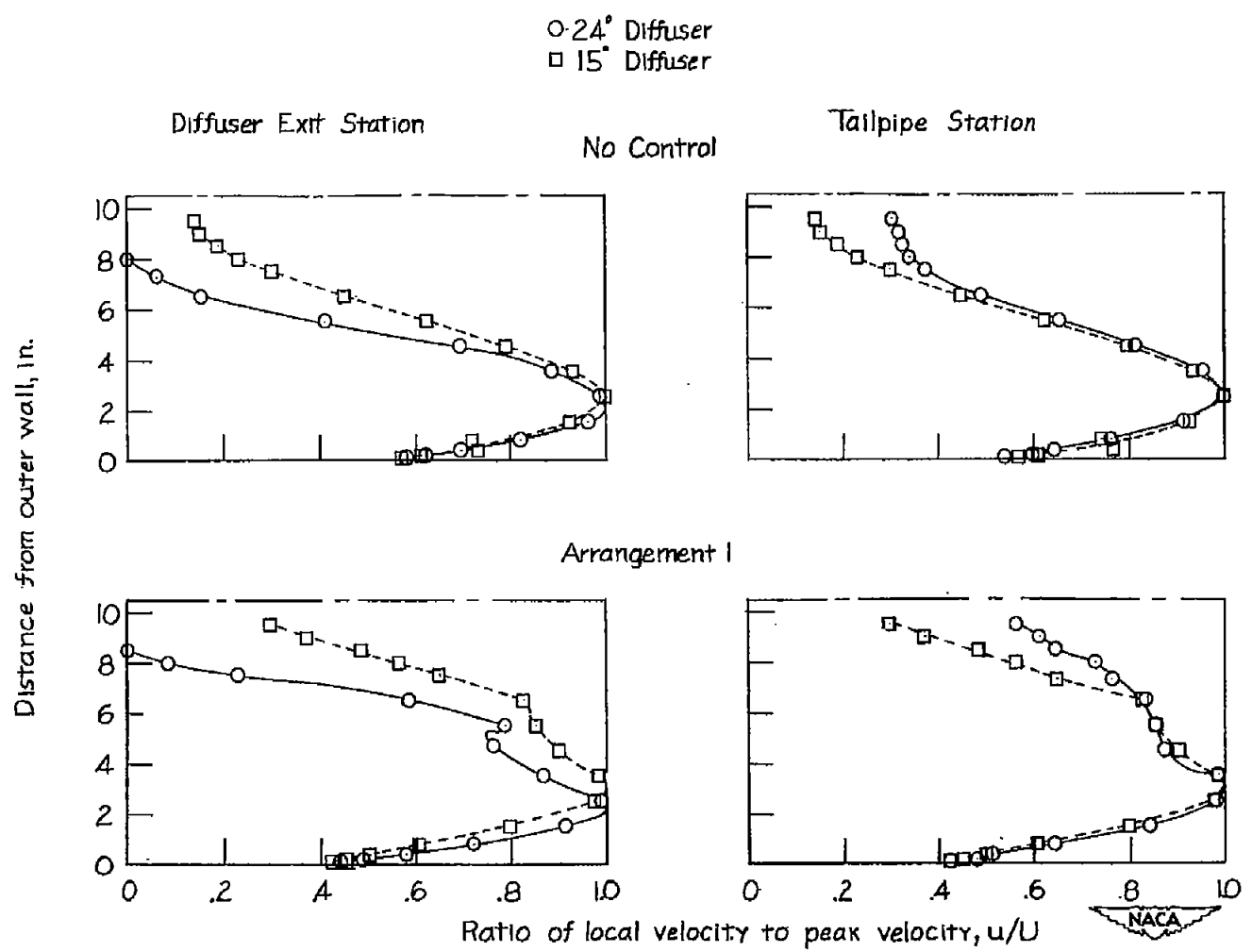


Figure 9.- Comparison of the 15° and 24° diffuser velocity profiles at both the diffuser exit and tailpipe stations for no control and the best control configuration.  $\bar{x}_1 = 0^{\circ}$ ;  $\bar{p}_1/\bar{p}_{1a} \approx 0.95$ .

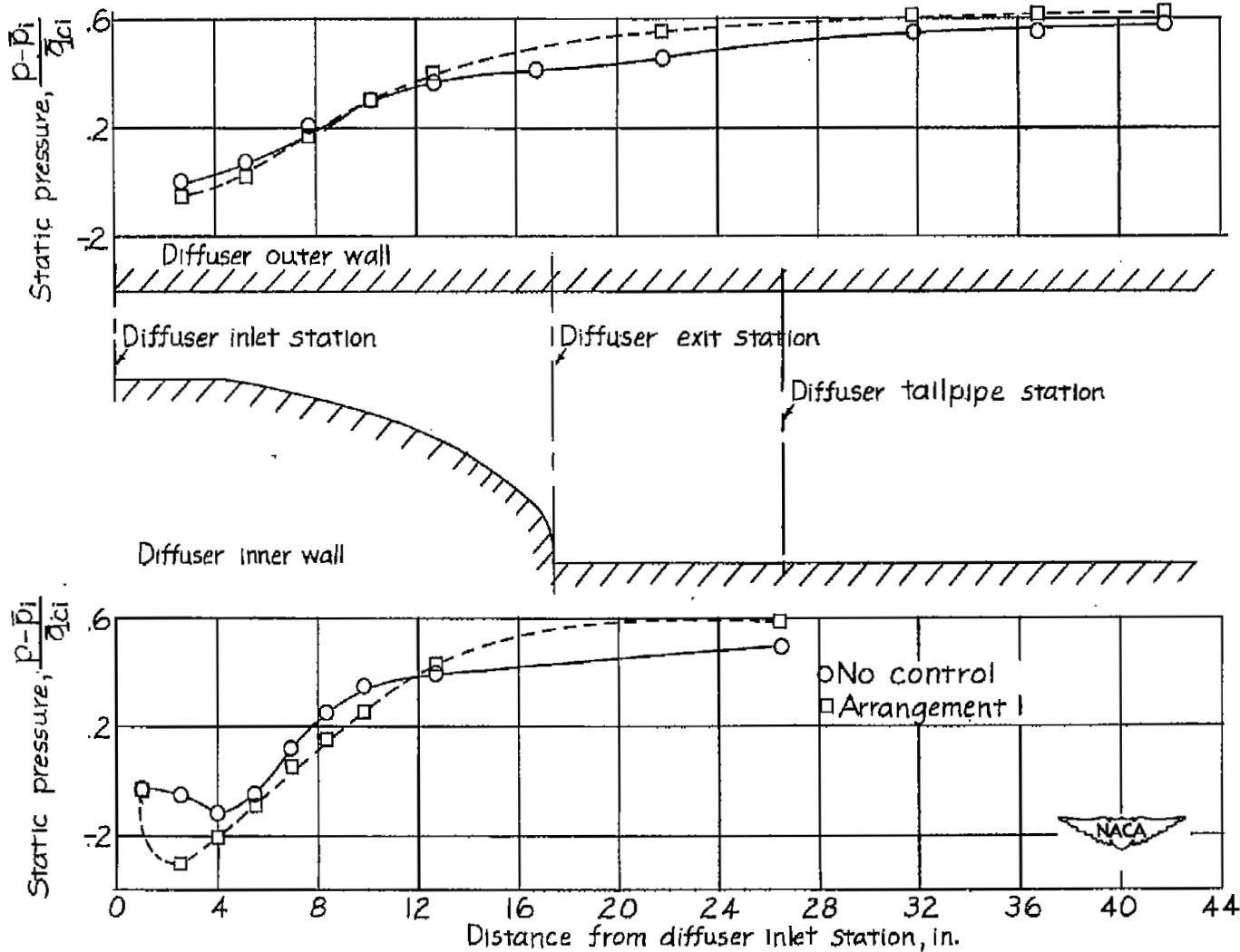


Figure 10.- Variation of the static pressure on both the inner and outer walls of the diffuser.  $\bar{\alpha}_1 = 0^\circ$ ;  $\bar{p}_1/\bar{p}_{1a} \approx 0.95$ .

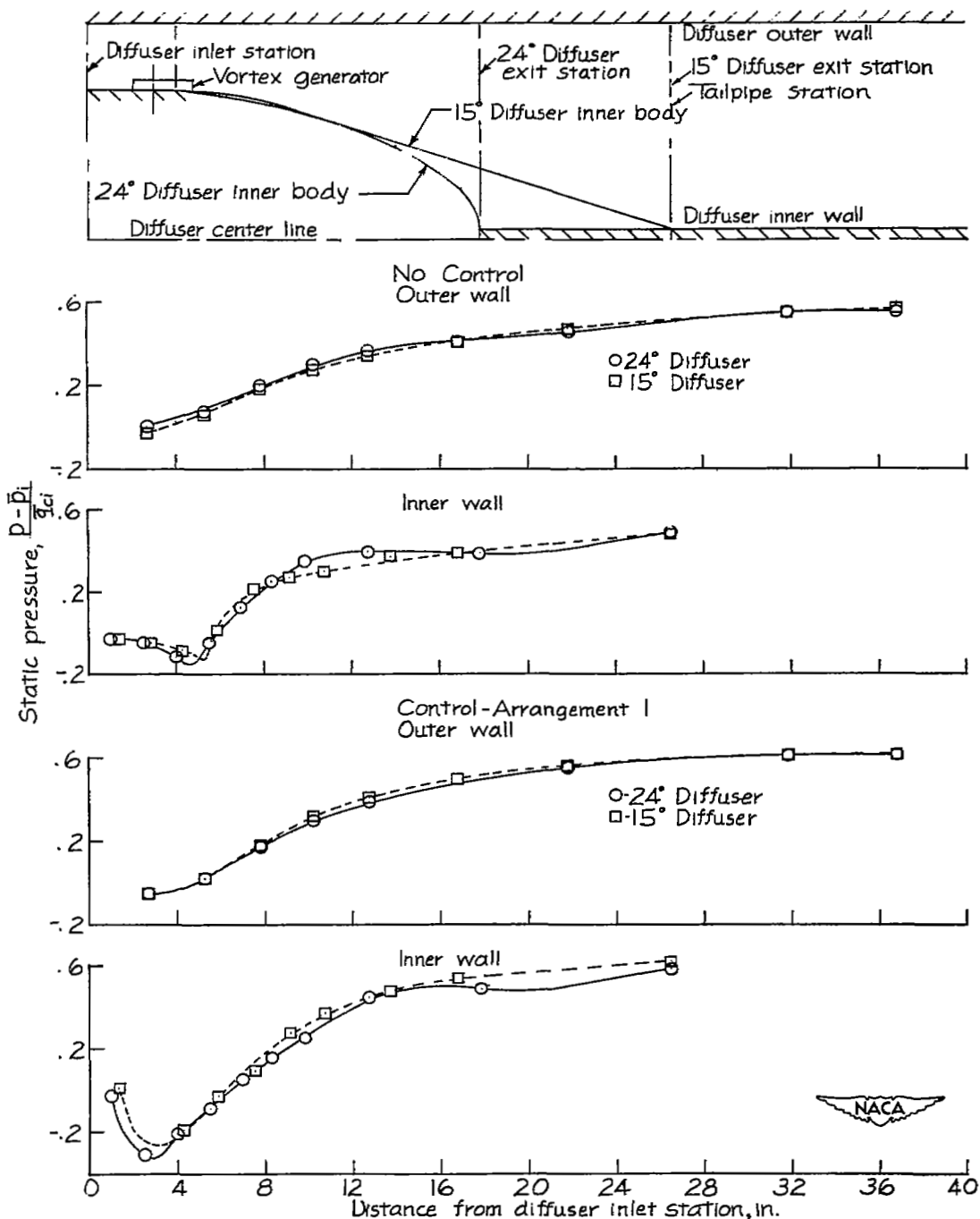


Figure 11.- Comparison of the 15° and 24° diffuser longitudinal static-pressure distributions along both the diffuser outer and inner walls for no control and for the best control configuration.  $\bar{\alpha}_1 = 0^\circ$ ;  $\bar{P}_1/\bar{P}_{1a} \approx 0.95$ .

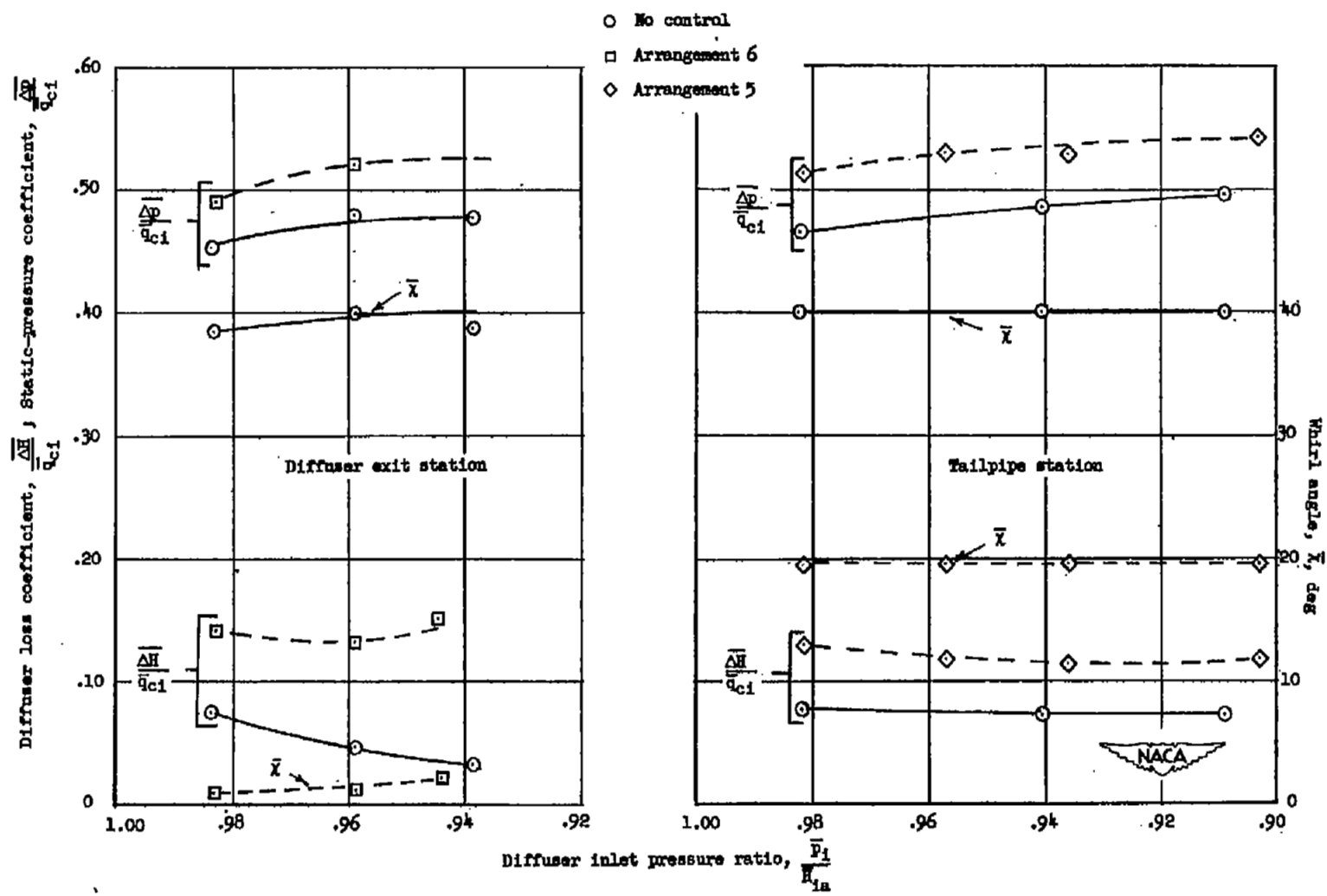


Figure 12.- Variation of the static-pressure coefficient, loss coefficient, and whirl angle at both the tailpipe and diffuser exit stations with inlet pressure ratio.  $\bar{\alpha}_1 = 20.6^\circ$ .

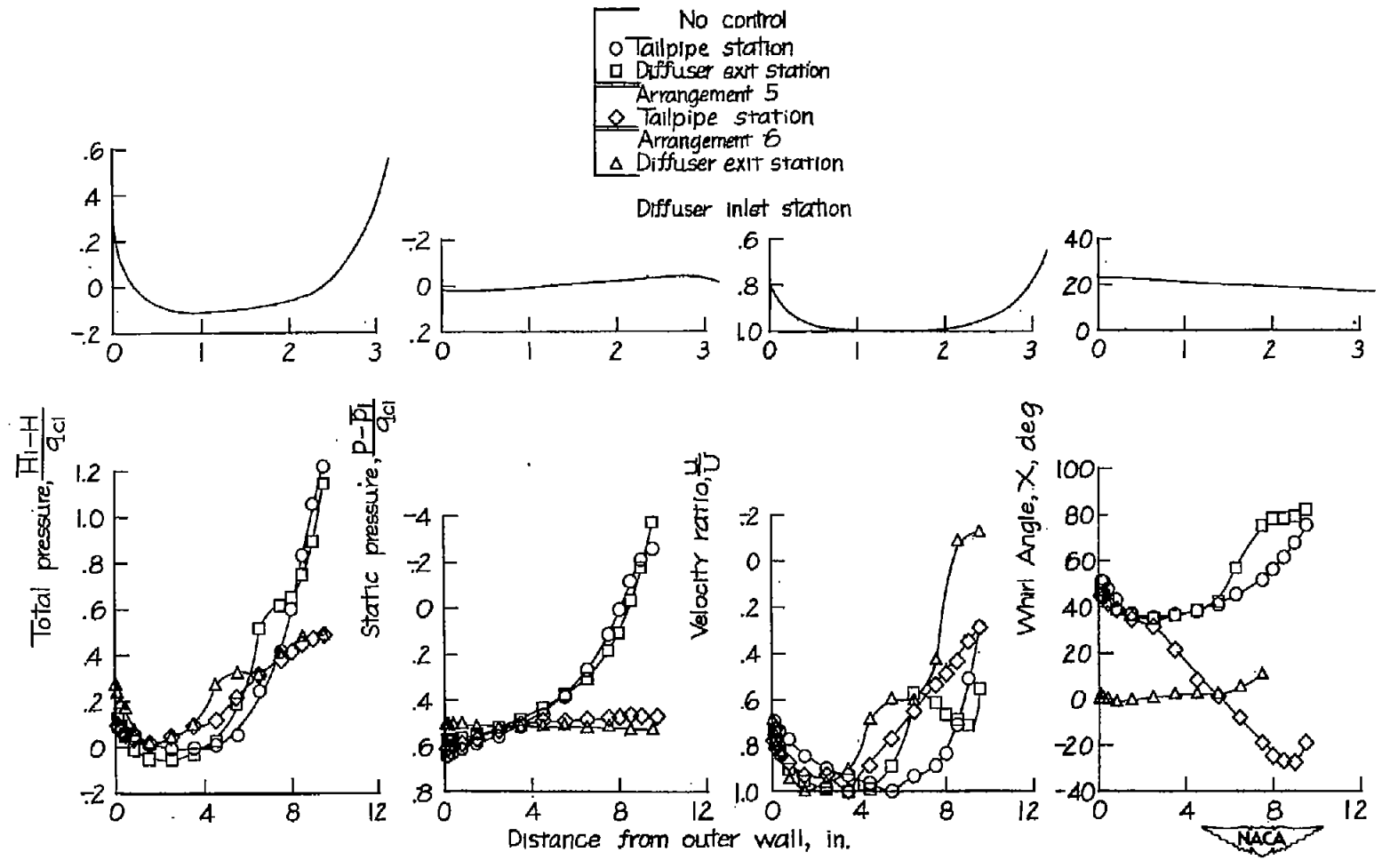


Figure 13.- Radial variation of total pressure, static pressure, velocity ratio, and whirl angle at both the tailpipe and diffuser exit stations.  $\bar{\alpha}_1 = 20.6^\circ$ ;  $\bar{p}_1/\bar{H}_{1a} \approx 0.95$ .

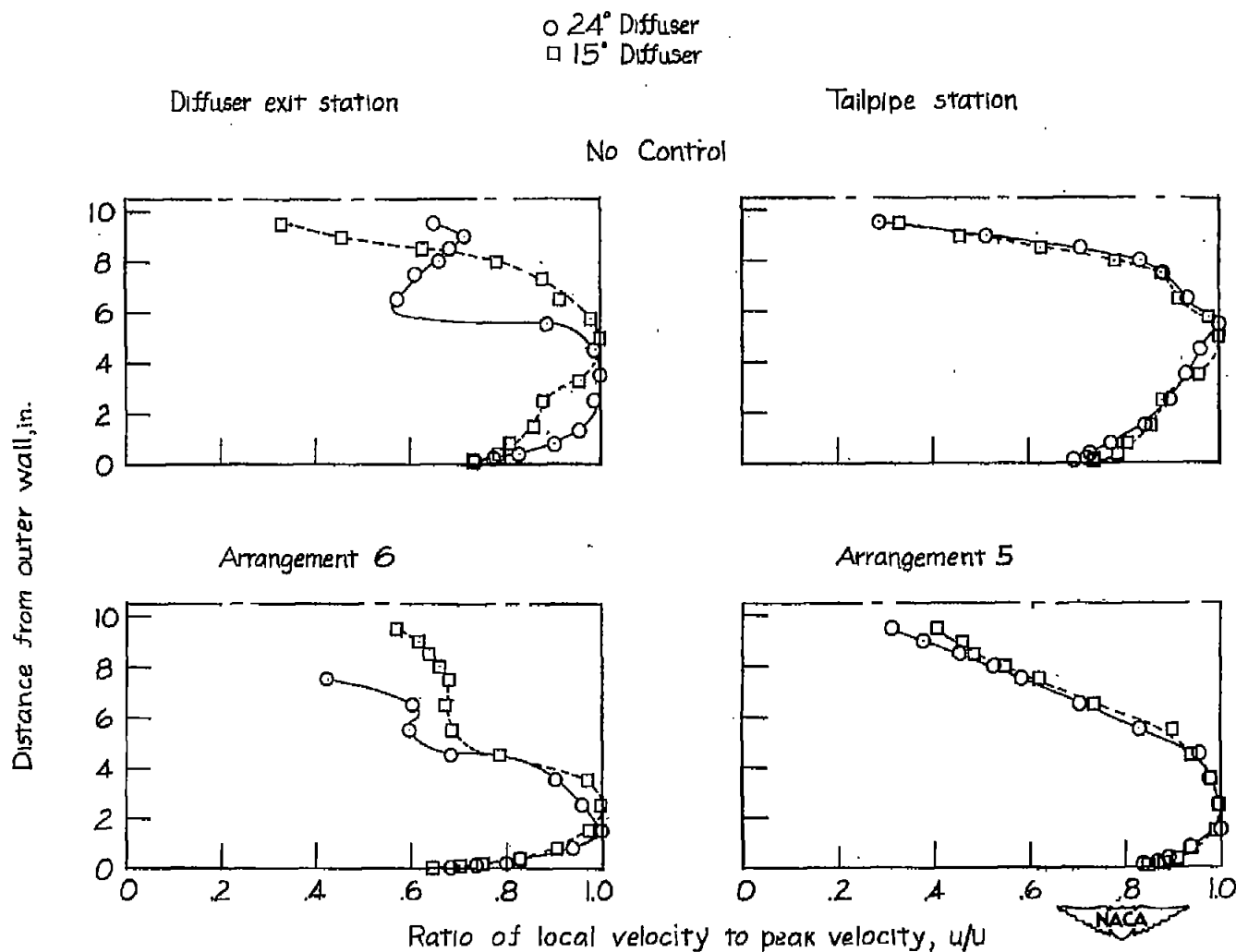


Figure 14.- Comparison of the 15° and 24° diffuser velocity profiles at the diffuser exit and tailpipe stations for no control and for two control configurations.  $\bar{x}_1 = 20.6^\circ$ ;  $\bar{p}_1/\bar{H}_{1a} \approx 0.95$ .

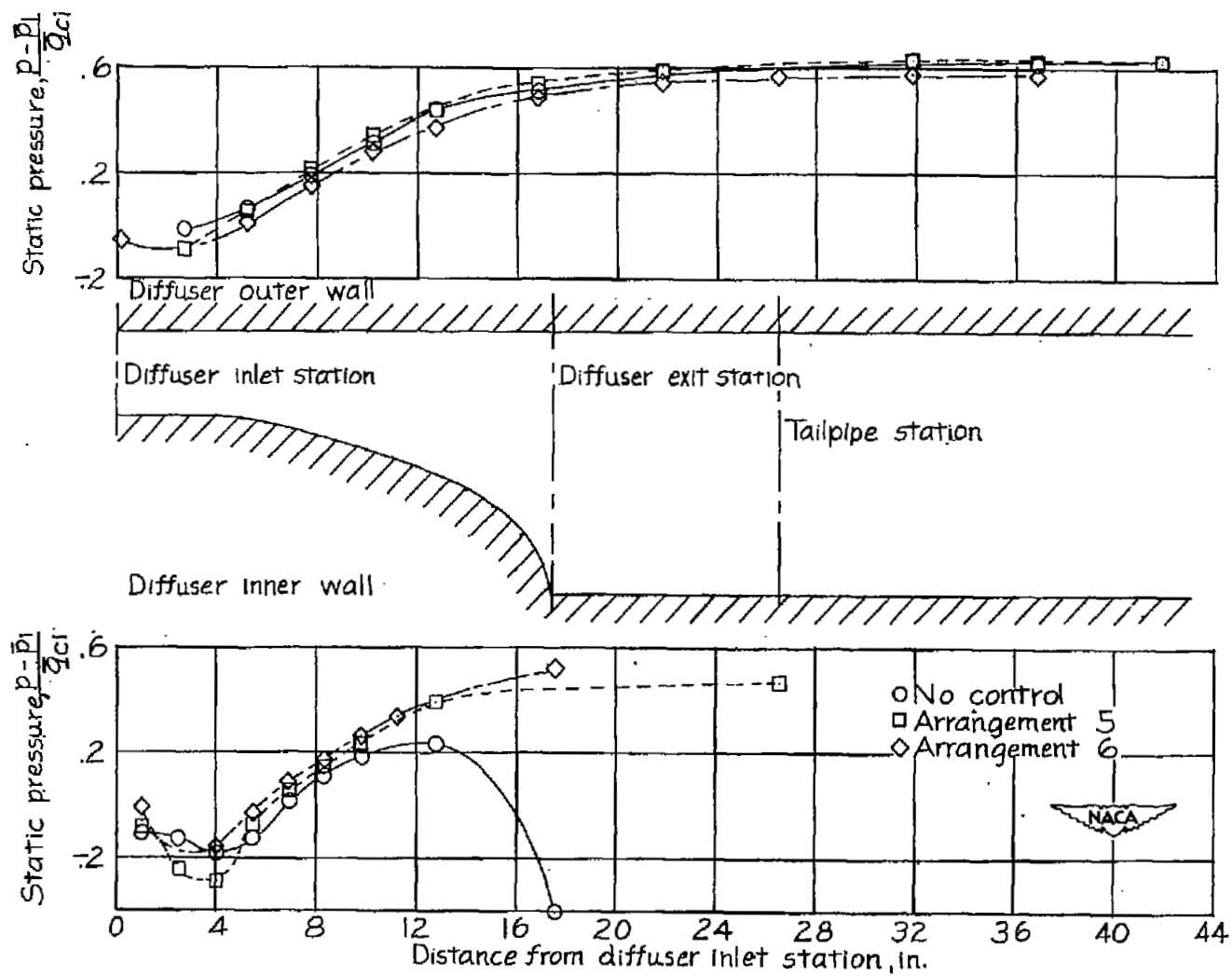


Figure 15.- Variation of the static pressure on both the inner and outer walls of the diffuser.  $\bar{\chi}_1 = 20.6^\circ$ ;  $\bar{p}_1/\bar{H}_{1a} \approx 0.95$ .

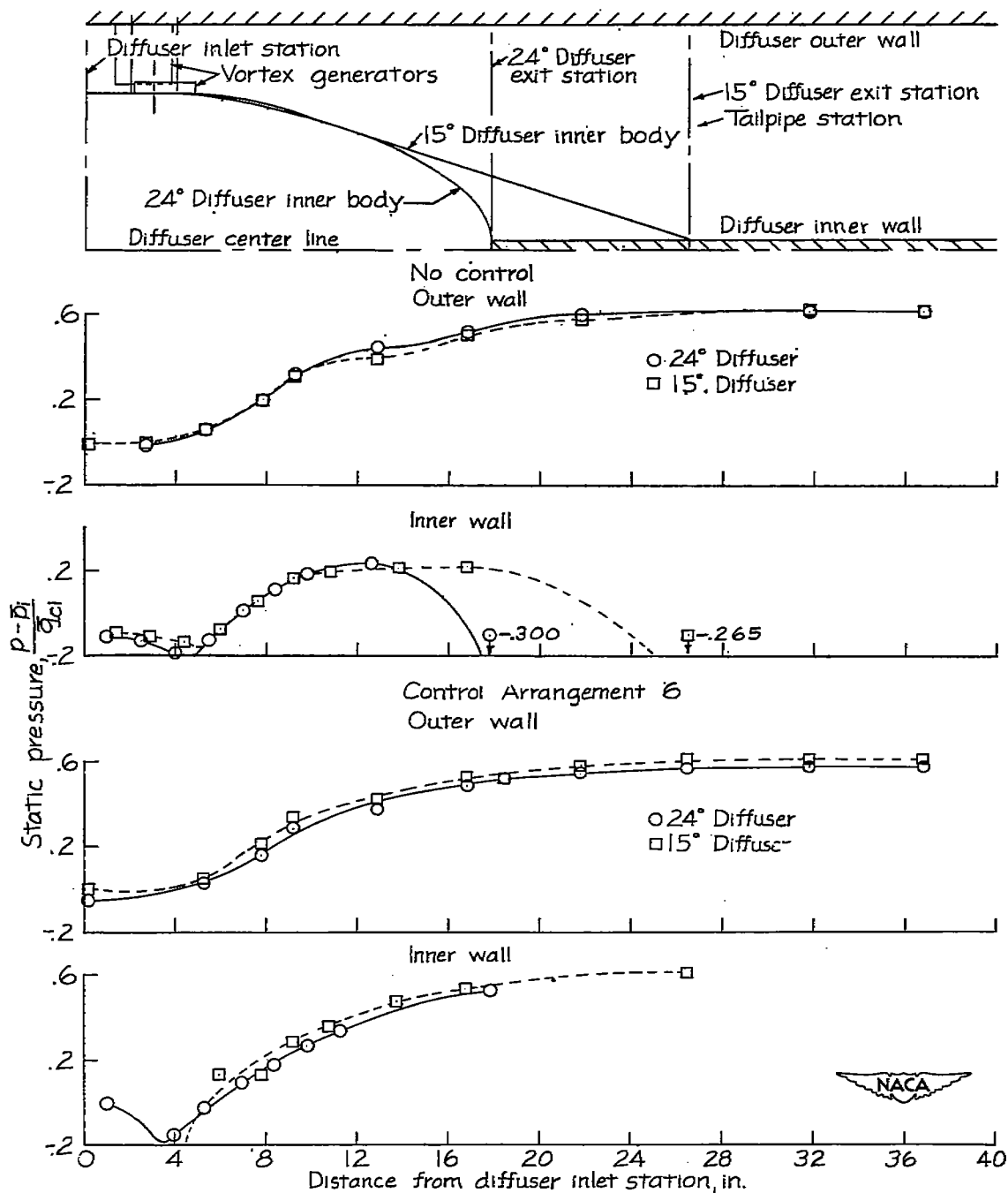


Figure 16.- Comparison of the 15° and 24° diffuser longitudinal static-pressure distributions along both the diffuser outer and inner walls for no control and for a control configuration.  $\bar{x}_1 = 20.6^\circ$ ;  
 $\bar{p}_1 / \bar{p}_{1a} \approx 0.95$ .

# SECURITY INFORMATION

NASA Technical Library



3 1176 01438 0092

